Molybdenum-Mediated Oxygen Atom Transfer: An Improved Analogue Reaction System of the Molybdenum Oxotransferases

**Brian E. Schultz,[1] Stephen F. Gheller, Mark C. Muetterties, Michael J. Scott, and R. H. Holm***

Contribution from the Department of Chemistry, Harvard University, Cambridge, Massachusetts 02138

Received October 28, 1992

Abstract: A new oxo transfer reaction system of relevance to the molybdenum oxotransferase group of enzymes has been developed. A set of ligands and their sterically hindered $Mo^{VI}O_2$ complexes have been prepared: $MoO_2(L\text{-}NO)_2$, $MoO_2(tBuL\text{-}NO)_2$, $MoO_2(L\text{-}NS)_2$, and $MoO_2(tBuL\text{-}NS)_2$ (L-NO = diphenyl-2-pyridylmethanolate(1−), $tBuL\text{-}NO$ = bis(4-*tert*-butylphenyl)-2-pyridylmethanolate(1−), L-NS = diphenyl-2-pyridylmethanethiolate(1−), $tBuL\text{-}NS$ = bis-(4-*tert*-butylphenyl)-2-pyridylmethanethiolate(1−)). Structures of $MoO_2(L\text{-}NO)_2$, $MoO_2(tBuL\text{-}NO)_2$, and MoO_2-($tBuL\text{-}NS)_2$ (**3**) reveal frontside steric hindrance of the MoO_2 units. Complex **3**, prepared in 98% yield, has a distorted octahedral structure with trans sulfur ligands and two *p-tert*-butylphenyl groups disposed so as to impede $Mo^V\text{-}O\text{-}Mo^V$ bridge formation. Reaction of **3** with Et_3P in THF affords the $Mo^{IV}O$ complex $MoO(tBuL\text{-}NS)_2$ (**4**, 69%), which has a distorted trigonal bipyramidal structure with an $MoOS_2$ equatorial plane. The complexes **3**/**4** are the essential components of the newly developed oxo transfer analogue reaction system: $3 + X \rightleftharpoons 4 + XO$. The equilibrium $3 + 4 \rightleftharpoons Mo_2O_3(tBuL\text{-}NS)_4$ with $K_{eq} = 63(7)$ M^{-1} was demonstrated in benzene solution, but the μ-oxo Mo^V species was found to be absent in reaction systems in other solvents. The system **3**/**4** has been shown to oxidize or reduce some 15 substrates X/XO including the types X = tertiary phosphine and XO = As-oxide, Se-oxide, S-oxide, heterocyclic N-oxides, and tertiary amine N-oxides. Among these are five enzyme substrates. With use of ^{18}O-labeled complexes and substrates, it was demonstrated that reactions in this system proceed by oxygen atom transfer; i.e., the atom transferred originates in the substrate or the oxo-Mo group. In terms of our reactivity scale for oxo transfer, **4** is thermodynamically competent to reduce XO in reaction couples X/XO with $\Delta H \geq -43$ kcal/mol and bond energy $D_{X\text{-}O}$ < 103 kcal/mol. Compared to other oxo transfer reaction systems developed in this laboratory and elsewhere, the current system presents the distinct advantages of structurally authenticated $Mo^{VI}O_2$ and $Mo^{IV}O$ components, stability to and reactivity with a much broader range of oxidized substrates, and sensitivity of reaction rates to variation of substrate. The results obtained here further support the oxo transfer mechanistic hypothesis as applied to enzymes whose active centers do not contain terminal sulfide or hydrosulfide ligands.

Introduction

We have proposed that a broad class of molybdenum enzymes[2] which catalyze the overall reaction $X + H_2O \rightleftharpoons XO + 2H^+ + 2e^-$ operate by the mechanism of the oxygen atom (oxo) transfer.[3,4] For enzymes such as sulfite oxidase[5] and DMSO reductase[6,7] that contain no sulfido terminal ligands at the active site, the oxo transfer hypothesis is expressed by the primary oxo transfer reaction[8] **1**, which results in the oxidation/reduction of substrate

$$Mo^{VI}O_2L_n + X \rightleftharpoons Mo^{IV}OL_n + XO \qquad (1)$$
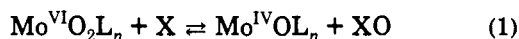
X/XO and implicates the dioxomolybdenum(VI) and oxomolybdenum(IV) functional groups in the process. Oxygen-18 isotope tracer experiments by Hille and Sprecher[9] have provided a key demonstration that the oxygen atom inserted in the substrate of xanthine oxidase originates at the molybdenum site and is not

directly derived from solvent water. Hence, this enzyme is one example of an oxotransferase.

In order to demonstrate the viability of molybdenum-mediated oxo transfer reactions, we have devised an oxo transfer system based on reaction 1 with L = $L\text{-}NS_2$ (2,6-bis(2,2-diphenyl-2-thioethyl)pyridinate(2−)), a hindered ligand employed with the intention of providing biologically relevant coordination (NS_2) and suppressing the formation of a μ-oxo Mo(V) dimer. This system has proven highly effective in atom transfer, sustaining clean oxidation and reduction of a variety of compounds,[10–14] including enzyme substrates such as biotin S-oxide, Me_2SO, and nitrate. However, this system has certain limitations. One or both complexes are unstable in the presence of sulfite and strong oxo donors such as tertiary amine N-oxides. While the structure of $MoO_2(L\text{-}NS_2)$ has been crystallographically demonstrated,[10] the oxomolybdenum(IV) complex has not been obtained as diffraction-quality crystals, so that its structure remains unestablished. Rate constants and activation enthalpies for reductions of substrates XO (N-oxides, S-oxides, nitrate) are essentially invariant with substrate[10,13,14] even though, among properties differing among substrates, X–O bond energies cover a range of

(1) National Science Foundation Predoctoral Fellow, 1989–1992.

(2) Bray, R. C. *Q. Rev. Biophys.* **1988,** *21,* 299.

(3) Holm, R. H.; Berg, J. M. *Acc. Chem. Res.* **1986,** *19,* 363.

(4) Holm, R. H. *Coord. Chem. Rev.* **1990,** *110,* 183. This article summarizes much of the biologically related molybdenum-mediated oxo transfer research of this laboratory.

(5) Hille, R.; Massey, V. In *Molybdenum Enzymes*; Spiro, T. G., Ed.; Wiley-Interscience: New York, 1985; Chapter 9.

(6) Bastian, N. R.; Kay, C. J.; Barber, M. J.; Rajagopalan, K. V. *J. Biol. Chem.* **1991,** *266,* 45.

(7) McEwan, A. G.; Ferguson, S. J.; Jackson, J. B. *Biochem. J.* **1991,** *274,* 305.

(8) Holm, R. H. *Chem. Rev.* **1987,** *87,* 1401.

(9) Hille, R.; Sprecher, H. *J. Biol. Chem.* **1987,** *262,* 10914.

(10) Berg, J. M.; Holm, R. H. *J. Am. Chem. Soc.* **1985,** *107,* 917, 925.

(11) Harlan, E. W.; Berg, J. M.; Holm, R. H. *J. Am. Chem. Soc.* **1986,** *108,* 6992.

(12) Caradonna, J. P.; Harlan, E. W.; Holm, R. H. *J. Am. Chem. Soc.* **1986,** *108,* 7856.

(13) Caradonna, J. P.; Reddy, P. R.; Holm, R. H. *J. Am. Chem. Soc.* **1988,** *110,* 2139.

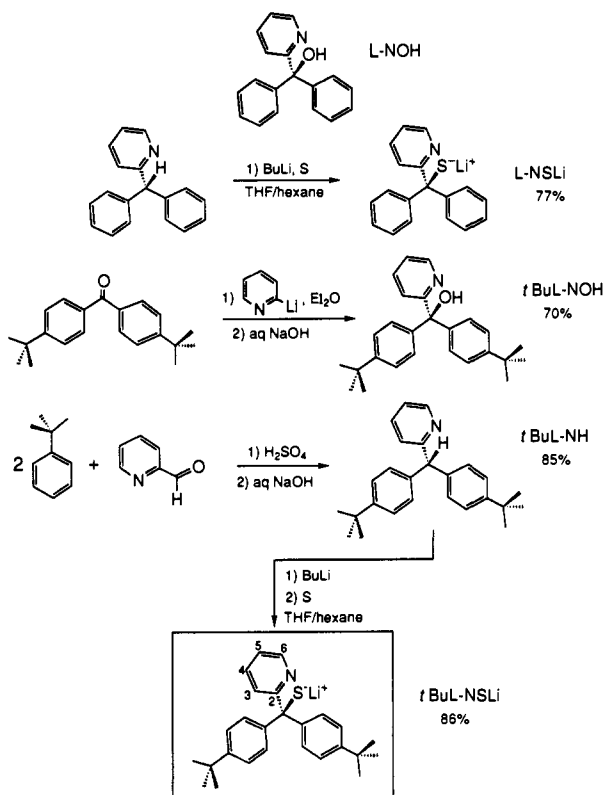(14) Craig, J. A.; Holm, R. H. *J. Am. Chem. Soc.* **1989,** *111,* 2111.

Figure 1. Summary of the methods used to prepare the ligands L-NSLi, *t*BuL-NOH, and *t*BuL-NSLi; yields are indicated. Ligand L-NOH has been previously reported.[19]

ca. 15 kcal/mol. Consequently, the kinetics data are not informative with respect to the nature of the atom transfer event itself.

We have sought an analogue reaction system in which the foregoing limitations are largely alleviated, the formation of a μ-oxo molybdenum(V) dimer (which complicates analysis of oxo transfer kinetics[15]) is suppressed, and a coordination sphere reasonably consistent with molybdenum EXAFS results[16] is preserved. Toward that end, we have prepared a series of bidentate ligands, based on the common fragment diphenyl-2-pyridylmethyl, which may be elaborated to provide nitrogen–oxygen/sulfur coordination. An appropriately substituted N–S ligand presents an extent of steric encumbrance sufficient to subdue μ-oxo dimer formation in systems capable of transforming by oxo transfer a broad variety of substrates. Certain leading results of this investigation have been briefly described.[17]

Experimental Section

Preparation of Compounds. Pyridine-2-aldehyde, diphenyl-2-pyridylmethane, triethylphosphine, phenylmagnesium bromide in ether, and *n*-butyllithium in hexane were commercial samples. 2-Bromopyridine was distilled and solvents were dried prior to use. All operations were performed under a pure dinitrogen atmosphere. Syntheses of ligands and complexes are outlined in Figures 1 and 2, respectively.

(a) **Ligands. Lithium Diphenyl-2-pyridylmethanethiolate (L-NSLi).** A solution of 23 mL (51 mmol) of 2.2 M *n*-butyllithium was added over 5–8 min to a stirred solution of 12.3 g (50 mmol) of diphenyl-2-pyridylmethane in 180 mL of THF at –60 °C. Elemental sulfur (1.6 g, 50 mmol) was added in a single portion and the stirring was continued at –60 °C for 45 min, over which time a precipitate appeared. The reaction mixture was stirred overnight as it warmed to ambient

(15) Reynolds, M. S.; Berg, J. M.; Holm, R. H. *Inorg. Chem.* **1984,** *23,* 3057.

(16) (a) George, G. N.; Kipke, C. A.; Prince, R. C.; Sunde, R. A.; Enemark, J. H.; Cramer, S. P. *Biochemistry* **1989,** *28,* 5075 and references therein. (b) George, G. N.; Cleland, W. E., Jr.; Enemark, J. H.; Smith, B. E.; Kipke, C. A.; Roberts, S. A.; Cramer, S. P. *J. Am. Chem. Soc.* **1990,** *112,* 2541.

(17) Gheller, S. F.; Schultz, B. E.; Scott, M. J.; Holm, R. H. *J. Am. Chem. Soc.* **1992,** *114,* 6934. The 6-H chemical shifts of **3** and **4** are inverted in this report.
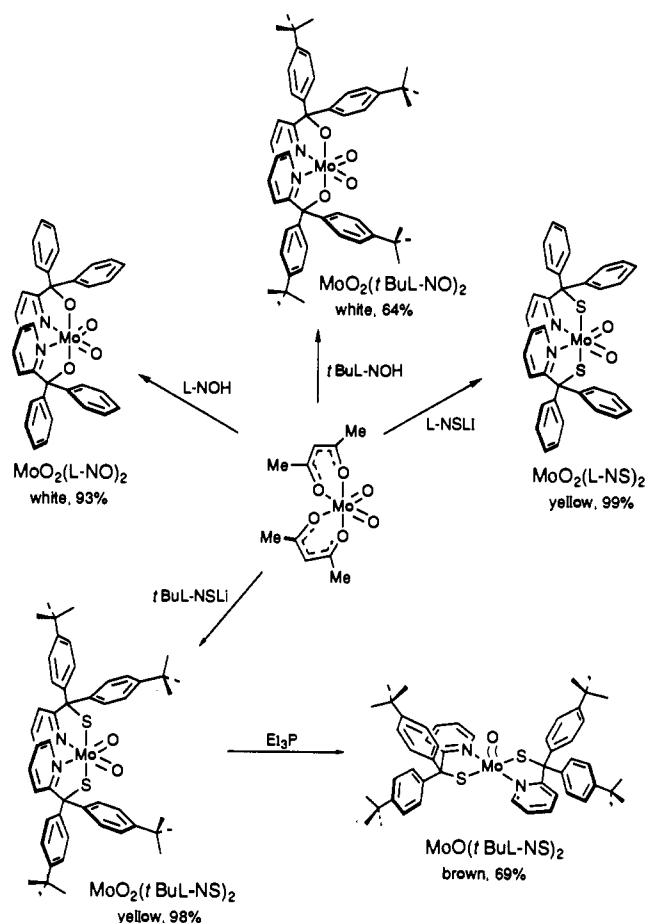

Figure 2. Schematic representation of the preparation of the Mo(VI) complexes MoO₂(L-NO)₂, MoO₂(*t*BuL-NO)₂, MoO₂(L-NS)₂, and MoO₂(*t*BuL-NS)₂ by ligand substitution of MoO₂(acac)₂ and the Mo(IV) complex MoO(*t*BuL-NS)₂ by reduction of MoO₂(*t*BuL-NS)₂; purified yields are indicated.

temperature and then was stirred for one additional day. The solid was collected, washed thoroughly with ether, and dried in vacuo to afford the product as 13.8 g (77%) of a white solid. ¹H NMR (Me₂SO-*d*₆, anion): δ 6.86 (t, 3), 6.96 (t, 4), 7.39 (t, 1), 7.46 (d, 4), 8.08 (d, 1), 8.25 (d, 1). The NMR spectrum and analytical data are consistent with the mono-THF solvate formulation. Anal. Calcd for C₂₂H₂₂LiNOS: C, 74.34; H, 6.24; Li, 1.95; N, 3.94; S, 9.02. Found: C, 73.92; H, 6.53; Li, 2.06; N, 3.90; S, 9.04.

Bis(4-tert-butylphenyl)-2-pyridylmethanol (*t*BuL-NOH). A solution of 29.4 g (100 mmol) of 4,4'-di-*tert*-butylbenzophenone[18] in 200 mL of ether was added dropwise to a solution of 2-lithiopyridine (from 0.13 mol of 2-bromopyridine and *n*-butyllithium) in 220 mL of ether at –65 °C. The addition was made over 1 h and the temperature was maintained below –60 °C. The dark reaction mixture was stirred overnight, hydrolyzed with water, neutralized with NaOH, and extracted several times with ether. The solid obtained by removal of ether from the combined extracts was washed with cold methanol. This material was recrystallized from methanol to afford the product in 70% yield as a white solid; mp 168–170 °C. ¹H NMR (CDCl₃): δ 1.27 (s, 18), 6.18 (br s, 1), 7.12 (d, 1), 7.17 (m, 5), 7.29 (d, 4), 7.63 (t, 1), 8.56 (d, 1). Anal. Calcd for C₂₆H₃₁NO: C, 83.60; H, 8.37; N, 3.75. Found: C, 83.44; H, 8.36; N, 3.70.

Bis(4-*tert*-butylphenyl)-2-pyridylmethane (*t*BuL-NH). To a mixture of 26.8 g (0.25 mol) of pyridine-2-aldehyde and 77.4 mL (0.50 mol) of *tert*-butylbenzene was added dropwise 80 mL of concentrated H₂SO₄. The mixture was stirred overnight and was carefully neutralized with a solution of 116 g (2.90 mol) of NaOH in 300 mL of water. The resulting white solid was extracted into ether. The extracts were dried (Na₂SO₄) and filtered, and the combined filtrates were reduced to dryness in vacuo. The solid residue was recrystallized from methanol to afford the product as 76.2 g (85%) of white solid; mp 105–107 °C. ¹H NMR (CDCl₃): δ

(18) (a) Larner, B. W.; Peters, A. T. *J. Chem. Soc.* **1952,** 680. (b) Buu-Hoi, N. P.; Royer, R.; Xuong, N. D.; Thang, K. V. *Bull. Soc. Chim. Fr.* **1955,** 1204.

2716 *J. Am. Chem. Soc., Vol. 115, No. 7, 1993*

Schultz et al.

1.27 (s, 18), 5.63 (br s, 1), 7.08 (m, 5), 7.28 (m, 5), 7.59 (t, 1), 8.57 (d, 1). Anal. Calcd for $C_{26}H_{31}N$: C, 87.34; H, 8.74; N, 3.92. Found: C, 87.57; H, 8.83; N, 3.89.

Lithium Bis(4-*tert*-butylphenyl)-2-pyridylmethanethiolate (*t*BuL-NS-Li). To a solution of 10.0 g (28.0 mmol) of *t*BuL-NH in THF at –65 °C was added dropwise 11.2 mL (28.0 mmol) of 2.5 M *n*-butyllithium in hexane. The solution assumed a deep red color. Elemental sulfur (0.90 g, 28 mmol) was added in one portion. The reaction mixture was stirred overnight as it warmed to ambient temperature. The white precipitate was collected and washed thoroughly with ether. The solid was dissolved in THF and filtered to remove any unreacted sulfur. The filtrate was reduced to dryness, washed thoroughly with ether, and dried in vacuo to afford the product as 11.3 g (86%) of a white crystalline solid. ^{1}H NMR (Me$_2$SO-d_6): δ 1.22 (s, 18), 6.85 (t, 1), 7.00 (d, 4), 7.36 (d, 4), 7.41 (t, 1), 8.09 (d, 1), 8.12 (d, 1). The NMR and analytical data are consistent with the mono-THF solvate formulation. Anal. Calcd for $C_{30}H_{38}LiNOS$: C, 77.05; H, 8.19; N, 3.00; S, 6.86. Found: C, 76.68; H, 8.46; N, 2.99; S, 6.81.

(b) Complexes. MoO$_2$(L-NO)$_2$ (1). A solution of 1.05 g (4.00 mmol) of diphenyl-2-pyridylmethanol[19] in 25 mL of methanol was added to a solution of 0.65 g (2.00 mmol) of MoO$_2$(acac)$_2$.[20] The solution changed from pale yellow to colorless, and soon thereafter a white precipitate was deposited. The mixture was stirred for 5 min; the solid was collected and washed with cold methanol to afford the product as 1.20 g (92%) of a white microcrystalline solid. IR (KBr): ν_{MoO} 922, 910, 898 cm^{-1}. ^{1}H NMR (CDCl$_3$): δ 6.65 (t, 1), 7.09 (d, 2), 7.19–7.39 (m, 7), 7.53–7.64 (m, 4). Anal. Calcd for $C_{36}H_{28}MoN_2O_4$: C, 66.67; H, 4.35; N, 4.32. Found: C, 66.61; H, 4.29; N, 4.20.
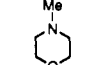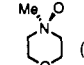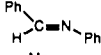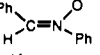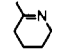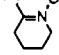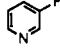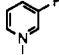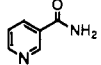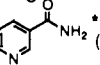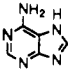
MoO$_2$(*t*BuL-NO)$_2$ (2). This compound was prepared according to the procedure for MoO$_2$(L-NO)$_2$ but with use of *t*BuL-NOH and was isolated in 64% yield as a white microcrystalline solid. IR (KBr): ν_{MoO} 922, 905 cm^{-1}. ^{1}H NMR (Me$_2$SO): δ 1.34 (s, 9), 6.74 (t, 1), 6.88 (d, 1), 7.32–7.46 (m, 8), 7.53 (d, 1), 7.86 (t, 1).

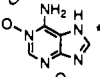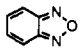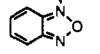**MoO$_2$(L-NS)$_2$.** To a solution of 1.63 g (5.00 mmol) of MoO$_2$(acac)$_2$ in 75 mL of methanol was added a solution of 4.30 g (12.0 mmol) of L-NSLi in 50 mL of methanol. The initial pale yellow color soon deepened and a copious yellow precipitate separated. The mixture was stirred for 1 h and filtered, and the solid was washed thoroughly with methanol and dried in vacuo. The product was obtained in quantitative yield as a yellow microcrystalline solid. IR (KBr): ν_{MoO} 920, 892, 884 cm^{-1}. ^{1}H NMR (CD$_2$Cl$_2$): δ 6.93 (d, 1), 7.08 (t, 1), 7.15–7.35 (m, 10), 7.64 (t, 1), 9.46 (d, 1). Anal. Calcd for $C_{36}H_{28}MoN_2O_2S_2$: C, 63.54; H, 4.15; N, 4.12; S, 9.42. Found: C, 65.05; H, 4.32; N, 3.91; S, 10.67.

MoO$_2$(*t*BuL-NS)$_2$ (3). A solution of 2.85 g (6.00 mmol) of *t*BuL-NSLi in 50 mL of methanol was added to a solution of 0.98 g (3.00 mmol) of MoO$_2$(acac)$_2$ in an equal volume of methanol. The initial pale yellow color intensified and a yellow precipitate appeared midway through the addition. The mixture was stirred for 1 h and the solid was collected and washed with methanol (2 × 10 mL). This material was dried in vacuo, giving 2.65 g (98%) of pure product as a yellow microcrystalline solid. Absorption spectrum (DMF): λ_{max} (ϵ_M) 371 (6220) nm. IR (KBr): ν_{MoO} 936, 901 cm^{-1}. ^{1}H NMR (CD$_2$Cl$_2$): δ 1.29 (s, 9), 1.33 (s, 9), 6.92 (d, 1), 6.97 (t, 1), 7.01 (d, 2), 7.18 (d, 2), 7.25–7.29 (m, 4), 7.58 (t, 1), 9.43 (d, 1). Anal. Calcd for $C_{52}H_{60}MoN_2O_2S_2$: C, 69.00; H, 6.68; N, 3.10; S, 7.08. Found: C, 69.23; H, 6.72; N, 3.07; S, 6.93.

MoO(*t*BuL-NS)$_2$ (4). A solution of 3.11 g (3.44 mmol) of MoO$_2$-(*t*BuL-NS)$_2$ in 125 mL of THF was treated with 0.76 mL (5.14 mmol) of Et$_3$P. The solution was refluxed for 5 h and the volatiles were removed in vacuo. The brown residue was washed thoroughly with acetonitrile (to remove Et$_3$PO) and was recrystallized from dichloromethane/hexane to give the pure product as 2.11 g (69%) of brown solid. Absorption spectrum (DMF): λ_{max} (ϵ_M) 328 (5210), 430 (3840), 518 (780), 700 (460) nm. IR (KBr): ν_{MoO} 943 cm^{-1}. ^{1}H NMR (CD$_2$Cl$_2$): δ 1.27 (s, 9), 7.21, (d, 2), 7.25–7.27 (q, 4), 7.41 (d, 2), 7.64 (d, 1), 7.70 (t, 1), 8.21 (t, 1), 9.37 (d, 1). Anal. Calcd for $C_{52}H_{60}MoN_2OS_2$: C, 70.25; H, 6.80; N, 3.15; O, 1.80; S, 7.21. Found: C, 70.05; H, 6.75; N, 3.01; O, 1.91; S, 7.07.

(c) Substrates. With reference to Figure 3, the amine N-oxide 7,[21] the nitrones 9[22] and 10,[23] the arylamine N-oxides 11,[24] 13,[25] and the

$$\text{MoO}_2(t\text{BuL-NS})_2 + X \xrightleftharpoons[\text{DMF}] \text{MoO}(t\text{BuL-NS})_2 + XO$$

X	XO	% yield
Et$_3$P (5)	Et$_3$PO	98
Me$_3$N	Me$_3$NO· (6)	93
(PhCH$_2$)$_3$N	(PhCH$_2$)$_3$NO (7)	87
(8)	(8)	92
(9)	(9)	87
(10)	(10)	96
(11)	(11)	82
(12)	(12)	86
(13)	(13)	88
(14)	(14)	85
Me$_2$S	Me$_2$SO· (15)	81
Ph$_2$S	Ph$_2$SO· (16)	89
Ph$_2$Se	Ph$_2$SeO (17)	94
Ph$_3$As	Ph$_3$AsO (18)	90
IO$_3^-$	IO$_4^-$· (19)	~100%

*enzyme substrate

Figure 3. Transformations of substrates 1–15 and in situ yields in the indicated oxo transfer reaction system. The majority of reactions were performed with stoichiometric amounts of substrate and complex.

selenoxide 17[26] were prepared by literature procedures. The remaining substrates were commercial samples and were used as received.

^{18}O-Labeling Experiments. Mo^{18}O$_2$(*t*BuL-NS)$_2$ was prepared by stirring a solution of 80.0 mg (0.088 mmol) of the unlabeled compound in 10 mL of THF containing 50 μL of H$_2$^{18}O (Icon Services, Inc.; 96% enriched) for 36 h. The enriched compound was isolated by removal of solvent in vacuo and its identity was confirmed by ^{1}H NMR and FT-IR spectroscopy: ν_{MoO} (KBr) 887, 858. Attempts to label MoO(*t*BuL-NS)$_2$ in a similar system or in CH$_2$Cl$_2$ afforded extraneous signals in ^{1}H NMR spectra and were not pursued further.

(a) ^{18}O Transfer to Substrate. A solution of Mo^{18}O$_2$(*t*BuL-NS)$_2$ in 10 mL of THF was treated with 85 μL of a 1.04 mM solution of Et$_3$P (1.0 equiv) in THF and the reaction mixture was stirred for 36 h. Analysis of an aliquot by EI-MS demonstrated the formation of Et$_3$PO 63% enriched in ^{18}O. ^{1}H NMR integration of the 6-H signals of the Mo complexes obtained by solvent removal of an aliquot of the reaction mixture showed that the reaction was 93% complete at this point.

(b) ^{18}O Transfer from Substrate. A solution of 28.7 mg (0.032 mmol) of MoO(*t*BuL-NS)$_2$ and 7.45 mg (0.035 mmol) of Ph$_2$SO[27] 95% enriched in ^{18}O was stirred for 24 h. The solvent was removed in vacuo and the product Mo complex was shown to contain Mo^{16}O^{18}O(*t*BuL-NS)$_2$ by FD-MS. Integration of the 6-H signals of the Mo complexes showed the reaction to be >95% complete at this point.

X-ray Data Collection and Reduction. Colorless crystals of compounds 1 and 2 were grown by evaporation of dichloromethane/methanol solutions. Orange crystals of compound 3 were obtained by vapor diffusion of ether into a saturated solution in dichloromethane. Brown crystals of 4 resulted from the slow cooling of a saturated acetonitrile solution to –20 °C. Single crystals of all four compounds were coated with grease, attached to glass fibers, and transferred to a Nicolet P3F diffractometer equipped with a low-temperature device. Lattice parameters were obtained from a least-squares analysis of 25 machine-centered reflections with 20° ≤

(19) Markgraf, J. H.; Berryhill, S. R.; Groden, L. R.; Hensley, W. M.; Spence, G. G.; McMurray, W. J. *J. Org. Chem.* **1975**, *40*, 417.

(20) Chakravorti, M. C.; Bandyopadhyay, D. *Inorg. Synth.* **1992**, *29*, 129. acac = acetylacetonate(1–).

(21) Cristol, S. J.; Imhoff, M. A.; Lewis, D. C. *J. Org. Chem.* **1970**, *35*, 1721.

(22) Wheeler, O. H.; Gore, P. H. *J. Am. Chem. Soc.* **1956**, *78*, 3363.

(23) (a) Mitsui, H.; Zenki, S.; Shiota, T.; Murahashi, S.-I. *J. Chem. Soc., Chem. Commun.* **1984**, 874. (b) Murahashi, S.-I.; Shiota, T. *Tetrahedron Lett.* **1987**, 2383.

(24) Bellas, M.; Suschitzky, N. *J. Chem. Soc.* **1963**, 4007.

(25) Stevens, M. A.; Magrath, D. I.; Smith, H. W.; Braun, G. B. *J. Am. Chem. Soc.* **1958**, *80*, 2755.

(26) Krafft, F.; Vorster, W. *Chem. Ber.* **1893**, *26*, 2820.

(27) Okruszek, A. *J. Labelled Compd. Radiopharm.* **1983**, *20*, 741.

Table I. Crystallographic Data[a] for $MoO_2(L\text{-}NO)_2$ (**1**), $MoO_2(tBuL\text{-}NO)_2\cdot Solvate^b$ (**2**), $MoO_2(tBuL\text{-}NS)_2\cdot CH_2Cl_2$ (**3**), and $MoO(tBuL\text{-}NS)_2\cdot 3MeCN$ (**4**)

	1	2	3	4
formula	$C_{36}H_{28}MoN_2O_4$	$C_{52}H_{60}MoN_2O_4{}^{b,c}$	$C_{53}H_{62}Cl_2MoN_2O_2S_2$	$C_{58}H_{69}MoN_5OS_2$
formula wt	648.5	$936.0^{b,c}$	990.0	1012.2
space group	$C2/c$	$P2_1/n$	$C2/c$	$P2_1/n$
Z	4	4	4	4
a, Å	15.525(2)	17.206(6)	23.663(6)	14.998(3)
b, Å	13.048(3)	15.858(3)	17.993(3)	23.345(4)
c, Å	16.776(3)	19.668(3)	13.620(3)	15.892(3)
β, deg	118.75(2)	107.26(2)	118.41(1)	93.96(2)
V, Å^3	2979.4(9)	5125(2)	5101(2)	5551(2)
d_{calc}, g/cm^3	1.45	b	1.29	1.21
T, K	173	173	173	198
μ, mm^{-1}	0.48	b	0.48	0.35
R,[d] $R_w{}^e$ (%)	4.86, 5.38	6.47, 6.88	5.69, 6.21	6.38, 6.11

[a] All data collected with Mo Kα radiation ($\lambda = 0.71069$ Å). All compounds crystallize in the monoclinic system. [b] The crystal contained a disordered solvent molecule. See text for experimental details. [c] Unsolvated form. [d] $R = \Sigma ||F_o| - |F_c||/\Sigma|F_o|$. [e] $R_w = \{\Sigma[w(|F_o|^2 - |F_c|^2)]/\Sigma[w|F_o|^2]\}^{1/2}$.

$2\theta \leq 30°$. Decay corrections were based on the measured intensities of three reflections monitored periodically throughout the course of data collection; none of the compounds showed significant decay. The raw intensity data were converted to structure factor amplitudes and their esd's by correction for scan speed, background, and Lorentz and polarization effects using the program XDISK of the SHELXTL PLUS program package. Empirical absorption corrections based on the observed variations in intensity of azimuthal (Ψ) scans were applied to all data sets using the program XEMP. The four compounds crystallized in the monoclinic system. The systematic absences and statistics identified the space group as $C2/c$ for **1** and **3** and $P2_1/n$ for **2** and **4**. Crystallographic data are contained in Table I.

Structure Solutions and Refinements. The structures of the four compounds in Table I were solved by direct methods and were refined by means of standard least-squares and Fourier techniques. All non-hydrogen atoms were refined with anisotropic thermal parameters unless otherwise noted. Hydrogen atoms were assigned idealized locations and given a uniform value for B_{iso} of 0.8 Å^2. Compounds **1** and **3** both crystallize on the 2-fold position in the space group $C2/c$ with the asymmetric unit consisting of one-half of a molecule. In **3**, the asymmetric unit also contains a dichloromethane molecule which is disordered over a general position and was refined isotropically with a 0.5 occupancy factor. The asymmetric unit of **2** consists of one full $Mo^{VI}O_2$ molecule and a severely disordered region of solvate near the inversion center. The electron density in this area could not be fit to a chemically reasonable model; it was refined isotropically as six carbon atoms, three at full occupancy and three at a 0.5 occupancy factor. After the final stage of refinement, the largest peak in the difference Fourier map had a height of 1.4 e$^-$/Å^3 and was located in the solvate region. The ring carbon atoms of the phenyl groups were refined isotropically due to the small number of observed data. The asymmetric unit of **4** consists of a full metal complex and three solvent molecules which were refined isotropically. In the last cycles of refinement of the four structures, all parameters shifted by <1% of their esd's and, except for **2**, the final difference Fourier maps showed no significant electron density.[28]

Other Physical Measurements. Spectrophotometric and ^{1}H NMR measurements were performed under anaerobic conditions using standard instrumentation as described.[29] FT-IR spectra were measured with a Nicolet IR/42 instrument. Electron impact (EI) mass spectra were recorded using a JEOL AX-505 spectrometer; conditions were 3 keV ion energy and 70 eV electron ionization energy. Fast atom bombardment (FAB) mass spectra were obtained with a JEOL SX-102 instrument which utilized a Xe atom beam with 6 keV energy; the ion source energy was 10 keV. Field desorption (FD) mass spectra were measured with the JEOL AX-505 spectrometer; samples were deposited from solution on a carbon emitter. Conditions were 9 keV extraction potential, 3 keV ion energy, and a mass resolution of 1500.

Results and Discussion

Synthesis of Compounds. We have synthesized a series of ligands designed to reduce or eliminate the formation of a μ-oxo species by means of reaction 2 in the final analogue reaction

$$Mo^{VI}O_2L_2 + Mo^{IV}OL_2 \rightleftharpoons [Mo^VOL_2]_2O \qquad (2)$$
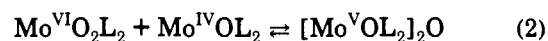
system. This series consists of N–O and N–S ligands containing the common diphenyl-2-pyridylmethyl fragment. The path to the components of the final reaction system proceeded through complexes with N–O ligands and then to those with N–S ligands, inasmuch as the former were initially much simpler to prepare and provided structural information of significant value in N–S ligand design. The efficacious synthesis described below for $tBuL\text{-}NS^-$, the ultimate ligand of choice, supplanted a five-step procedure by which the ligand was first prepared.

Ligand preparations, yields, and abbreviations are set out in Figure 1. Preparations are standard for the first four ligands. The most important ligand, $tBuL\text{-}NS^-$, is readily prepared in three steps from inexpensive precursors. Sequential attack of pyridine electrophiles in strong acid at the para carbon atom of *tert*-butylbenzene affords $tBuL\text{-}NH$, which upon lithiation and reaction with elemental sulfur yields the desired N–S ligand, readily isolated as its lithium salt. These ligands react smoothly with $MoO_2(acac)_2$ in methanol solutions to afford the corresponding set of $Mo^{VI}O_2$ complexes depicted in Figure 2. Treatment of $MoO_2(tBuL\text{-}NS)_2$ with 1.5 equiv of triethylphosphine in refluxing THF resulted in clean atom transfer and the formation of $MoO(tBuL\text{-}NS)_2$ in 69% purified yield. These two compounds are readily soluble in a variety of organic solvents such as DMF, acetonitrile, THF, and benzene. Note that all complexes contain *gem*-diphenyl groups that are positioned to provide a steric impediment to μ-oxo dimer formation. The inclusion of sulfur maintains a degree of consistency with molybdenum EXAFS analyses, which without exception indicate at least two ligand sulfur atoms in the coordination units of $Mo^{VI}O_2$ and $Mo^{IV}O$ states of the enzymes.[16] However, the ligand system obviously does not present dithiolene-type coordination which, based on the common structural component of the Mo-cofactors of these enzymes[30] and the resonance Raman spectrum of a DMSO reductase,[31] is the probable mode of metal binding.[32]

Structures. $Mo^{VI}O_2$ Complexes. The structures of three complexes of this type were established by X-ray methods. The first structure determined, that of $MoO_2(L\text{-}NO)_2$, presented in Figure 4, reveals the cis-dioxo distorted octahedral geometry with mutually trans anionic ligands common to nearly all structurally characterized five- and six-coordinate $Mo^{VI}O_2$ species. An imposed C_2 axis bisects the O(1)–Mo–O(1') angle. The disposition of the four phenyl rings places two of them toward the front of the molecule with a modest extension over the MoO_2 group

(28) See paragraph at the end of this article concerning supplementary material.

(29) Ciurli, S.; Carrié, M.; Weigel, J. A.; Carney, M. J.; Stack, T. D. P.; Papefthymiou, G. C.; Holm, R. H. *J. Am. Chem. Soc.* **1990**, *112*, 2654.
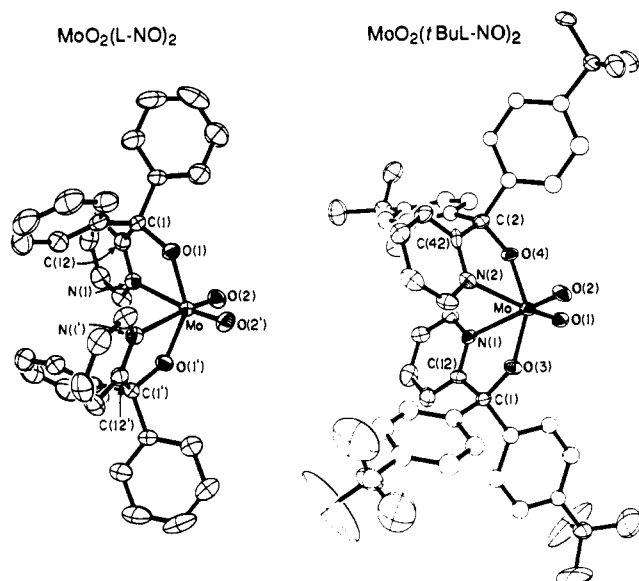
(30) (a) Rajagopalan, K. V.; Johnson, J. L. *J. Biol. Chem.* **1992**, *267*, 10199. (b) Rajagopalan, K. V. *Adv. Enzymol. Relat. Areas Mol. Biol.* **1991**, *64*, 215.

(31) Gruber, S.; Kilpatrick, L.; Bastian, N. R.; Rajagopalan, K. V.; Spiro, T. G. *J. Am. Chem. Soc.* **1990**, *112*, 8179.

(32) An alternative binding mode, using a pterin nitrogen and a dithiolene sulfur atom in a chelate structure, has been proposed: Fischer, B.; Strähle, J.; Viscontini, M. *Helv. Chim. Acta* **1991**, *74*, 1544.

MoO₂(L-NO)₂   MoO₂(*t*BuL-NO)₂

MoO₂(*t*BuL-NS)₂

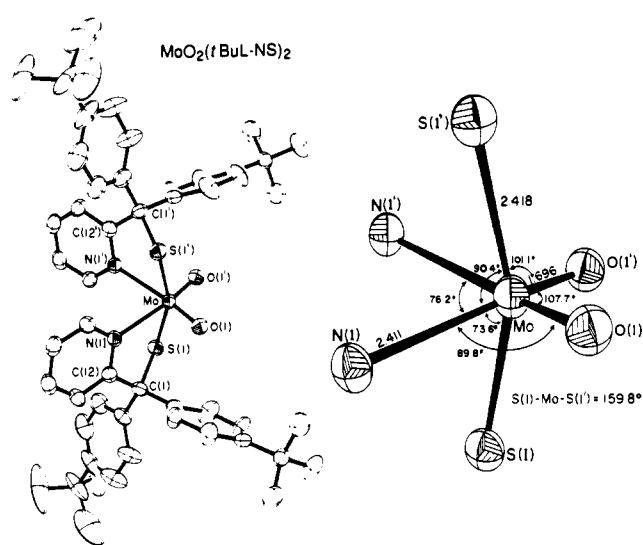**Figure 5.** The complete structure of MoO₂(*t*BuL-NS)₂ (left) showing the atom labeling scheme and 30% probability ellipsoids, and an expanded view of the coordination sphere with selected interatomic distances and angles (right). Primed and unprimed atoms are related by a C_2 axis.

Figure 4. The structures of MoO₂(L-NO)₂ and MoO₂(*t*BuL-NO)₂ showing the atom numbering schemes and 30% probability ellipsoids. Primed and unprimed atoms of MoO₂(L-NO)₂ are related by a C_2 axis. The phenyl rings of MoO₂(*t*BuL-NO)₂ were not refined anisotropically.

Table II. Selected Interatomic Distances (Å) and Angles (deg) for MoO₂(L-NO)₂ (1) and MoO₂(*t*BuL-NO)₂ (2)

	1		2
Mo–O(2)	1.704(3)	Mo–O(1)	1.710(8)
		Mo–O(2)	1.707(8)
Mo–O(1)	1.940(3)	Mo–O(3)	1.941(8)
		Mo–O(4)	1.946(8)
Mo–N(1)	2.363(4)	Mo–N(1)	2.359(8)
		Mo–N(2)	2.336(9)
O(2)–Mo–O(2')	103.1(7)	O(1)–Mo–O(2)	105.8(4)
		O(1)–Mo–N(1)	89.6(3)
N(1)–Mo–N(1')	92.0(2)	N(1)–Mo–N(2)	80.2(3)
O(2)–Mo–N(1)	83.4(1)	O(2)–Mo–N(2)	87.2(3)
		O(1)–Mo–O(4)	91.8(4)
O(2)–Mo–O(1)	105.5(1)	O(2)–Mo–O(4)	103.9(4)
N(1)–Mo–O(1)	71.9(1)	N(2)–Mo–O(4)	71.8(3)
		N(1)–Mo–O(4)	84.0(3)
		O(1)–Mo–O(3)	104.1(4)
O(2)–Mo–O(1')	96.5(1)	O(2)–Mo–O(3)	95.8(4)
		N(1)–Mo–O(3)	71.4(3)
		N(2)–Mo–O(3)	87.5(3)
O(1)–Mo–O(1')	144.5(2)	O(4)–Mo–O(3)	150.3(3)
Mo–O(1)–C(1)	129.1(3)	Mo–O(3)–C(1)	128.8(7)
		Mo–O(4)–C(2)	128.7(7)

Table III. Selected Interatomic Distances (Å) and Angles (deg) for MoO₂(*t*BuL-NS)₂

Mo–O(1)	1.696(4)	O(1)–Mo–S(1)	101.1(2)
Mo–S(1)	2.418(2)	N(1)–Mo–S(1)	73.6(2)
Mo–N(1)	2.411(5)	N(1')–Mo–S(1)	90.4(2)
O(1)–Mo–O(1')	107.7(3)	O(1)–Mo–S(1')	90.8(2)
O(1)–Mo–N(1)	89.8(2)	O(1)–Mo–N(1')	158.7(2)
N(1)–Mo–N(1')	76.2(2)	S(1)–Mo–S(1')	159.8(1)
		Mo–S(1)–C(1)	100.8(3)
		Mo–N(1)–C(12)	118.8(4)

in the conformation shown and directs the other two away from this group toward the rear of the molecule. The extent of steric hindrance appeared insufficient to prevent μ-oxo formation in this and related molecules. With this in mind and the desire to improve solubility properties, we then prepared MoO₂(*t*BuL-NO)₂. Its structure, also shown in Figure 4, has no imposed symmetry and is analogous to that of MoO₂(L-NO)₂. Comparison of dimensions in Table II reveals closely similar coordination units with the largest difference being compression of the N(1)–Mo–N(2) angle in MoO₂(*t*BuL-NO)₂ by 11.8°. The conspicuous departure of the trans O–Mo–O angles in the two molecules from the idealized 180° value presumably arises in part from Coulombic repulsion between terminal oxo and trans oxygen atoms. The frontside orientation of the two phenyl groups is maintained, with the *p-tert*-butyl substituents adding to the steric bulk. These observations indicated that the related N–S complex might be a suitable component of an analogue reaction system.

Both MoO₂(L-NS)₂ and MoO₂(*t*BuL NS)₂ were synthesized, but the former, as its oxygen counterpart, proved only slightly soluble and its structure was not determined. The structure of MoO₂(*t*BuL-NS)₂ is set out in Figure 5; metric data are contained in Table III. The molecule has an imposed C_2 axis that bisects

the O(1)–Mo–O(1') angle and a trans orientation of sulfur atoms. The distorted octahedral coordination unit possesses features related to the preceding two molecules and to other complexes with Mo^VIO₂N₂S₂ units,[33,34] in all of which the anionic sulfur atoms are trans. Among these features are trans S–Mo–S angles near 160°, indicating that substantial deviation from 180° is a general feature and not dependent on the ligand system. Comparison with MoO₂(*t*BuL-NO)₂ is revealing. The most important differences are a larger trans ligand angle S–Mo–S of 159.8(1)° vs the O–Mo–O angle of 150.3(3)°, a much longer Mo–S distance of 2.418(2) Å compared to the mean Mo–O value of 1.944 Å, and a less obtuse Mo–S–C angle of 100.8° in relation to the Mo–O–C angle of 128.8°. These differences effect a pronounced frontside projection of two *p-tert*-butylphenyl groups that is made readily apparent by the structural perspective in Figure 6. Here rings 2/2' overlie and extend well beyond the MoO₂ group and, in the observed conformation, form dihedral angles of 35.3° and 31.7° with each other and with the MoO₂ group, respectively. The other two such groups, containing rings 3/3', are disposed toward the back of the molecule and are oriented at a dihedral angle of 75.4°. Rings 2 and 3, with a dihedral angle of 78.4°, are roughly normal to each other. Clearly, MoO₂(*t*BuL-NS)₂ offers substantial frontside steric encumbrance to μ-oxo dimer formation, but as will be seen, formation of this species is possible under certain conditions.

(33) (a) Bruce, A.; Corbin, J. L.; Dahlstrom, P. L.; Hyde, J. R.; Minelli, M.; Stiefel, E. I.; Spence, J. T.; Zubieta, J. *Inorg. Chem.* **1982**, *21*, 917. (b) Berg, J. M.; Hodgson, K. O.; Bruce, A. E.; Corbin, J. L.; Pariyadath, N.; Stiefel, E. I. *Inorg. Chim. Acta* **1984**, *90*, 25. (c) Berg, J. M.; Spira, D.; Wo, K.; McCord, B.; Lye, R.; Co, M. S.; Belmont, J.; Barnes, C.; Kosydar, K.; Raybuck, S.; Hodgson, K. O.; Bruce, A. E.; Corbin, J. L.; Stiefel, E. I. *Inorg. Chim. Acta* **1984**, *90*, 35.
(34) (a) Dowerah, D.; Spence, J. T.; Singh, R.; Wedd, A. G.; Wilson, G. L.; Farchione, F.; Enemark, J. H.; Kristofzski, J.; Bruck, M. *J. Am. Chem. Soc.* **1987**, *109*, 5655. (b) Hinshaw, C. J.; Peng, G.; Singh, R.; Spence, J. T.; Enemark, J. H.; Bruck, M.; Kristofzski, J.; Merbs, S. L.; Ortega, R. G.; Wexler, P. A. *Inorg. Chem.* **1989**, *28*, 4483.
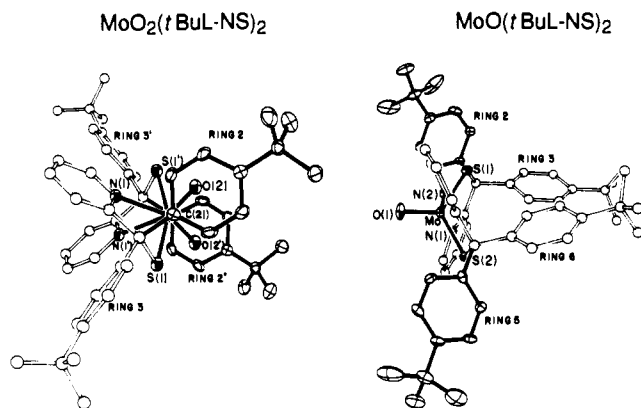
Molybdenum-Mediated Oxygen Atom Transfer

J. Am. Chem. Soc., Vol. 115, No. 7, 1993 2719

MoO₂(tBuL-NS)₂ — MoO₂(tBuL-NS)₂

MoO(tBuL-NS)₂ — MoO(tBuL-NS)₂

Figure 6. Perspectives of structures of MoO₂(tBuL-NS)₂ and MoO(tBuL-NS)₂ emphasizing the positions of *p-tert*-butylphenyl groups; those near or at the front of the molecule are shown with solid bonds while other groups and pyridyl rings have open bonds. MoO₂(tBuL-NS)₂ (left) is viewed down the C(21)–Mo–C(21′) direction; C(21,21′) are the ipso carbon atoms in rings 2,2′. The Mo atom is obscured by C(21). Primed and unprimed atoms are related by a C_2 axis.
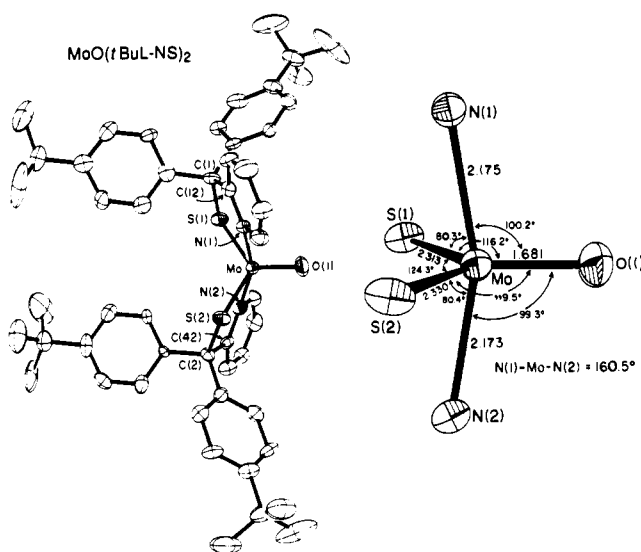
MoO(tBuL-NS)₂

Figure 7. The complete structure of MoO(tBuL-NS)₂ (left) showing the atom labeling scheme and 30% probability ellipsoids, and an expanded view of the coordination sphere with selected interatomic distances and angles (right).

Table IV. Selected Interatomic Distances (Å) and Angles (deg) for MoO(tBuL-NS)₂

Mo–O(1)	1.681(5)	O(1)–Mo–N(1)	100.2(3)
Mo–S(1)	2.313(3)	S(1)–Mo–N(1)	80.3(2)
Mo–S(2)	2.330(3)	S(2)–Mo–N(1)	89.1(2)
Mo–N(1)	2.175(7)	O(1)–Mo–N(2)	99.3(3)
Mo–N(2)	2.173(7)	S(1)–Mo–N(2)	92.1(2)
O(1)–Mo–S(1)	116.2(3)	S(2)–Mo–N(2)	80.4(2)
O(1)–Mo–S(2)	119.5(3)	N(1)–Mo–N(2)	160.5(3)
S(1)–Mo–S(2)	124.3(1)	Mo–S(1)–C(1)	105.2(3)
		Mo–S(2)–C(2)	105.1(3)
		Mo–N(1)–C(12)	123.9(6)
		Mo–N(1)–C(16)	116.8(5)

The structure of MoO(tBuL-NS)₂ is depicted in Figures 6 and 7 and bond distances and angles are compiled in Table IV. The molecule is best described in terms of a distorted trigonal bipyramidal stereochemistry with a MoOS₂ equatorial plane and two nitrogen atoms in axial positions. Bond angles in the plane are in the 116–124° range, N–Mo–S/O angles are 80–100°, and the N(1)–Mo–N(2) angle is 160.5(3)°, again indicating ligand repulsion by a terminal oxo atom. The equatorial atoms are essentially planar, with the molybdenum atom displaced from the O(1)S(1,2) plane by 0.012 Å in the direction of N(2). As

shown in Figure 6, *p-tert*-butylphenyl groups with rings 2/5 show very little frontside projection, leaving the MoO group rather exposed to attack, and rings 3/6 are thrust to the backside and approach coplanarity (dihedral angle 23.0°). Only two Mo^{IV}-ON₂S₂ complexes have been reported previously;[35] nothing is known about their structures or reactivities. The structures of some 12 five-coordinate Mo^{IV}O complexes that are not organometallic in nature and whose stereochemistry is not necessarily set by ligand constraints have been described.[36,37] All but one have a square or tetragonal pyramidal structure. The exception, MoO(SCH₂CH₂PPh₂)₂,[37] crystallizes with a stereochemistry intermediate between tetragonal pyramidal and trigonal bipyramidal, a circumstance approached by MoO(tBuL-NS)₂. In the latter, the Mo–O bond distance (1.681(5) Å) conforms closely to those of other Mo^{IV}O groups, while the mean Mo–S distance (2.322 Å) is the shortest reported for any Mo^{IV}O complex. Knowledge of the detailed structures of MoO₂(tBuL-NS)₂ and MoO(tBuL-NS)₂ permits identification of the dimensional changes pursuant to their interconversion by atom transfer. Other than MoO₂(S₂CNR₂)₂/MoO(S₂CNR₂)₂[36f,38a] and MoO₂(HB(3,5-Me₂pz)₃)η¹-S₂P(OEt)₂)/MoO(HB(3,5-Me₂pz)₃)(S₂P-(OEt)₂),[38b] the foregoing two complexes constitute the only Mo^{VI}O₂/Mo^{IV}O pair interconvertible by oxo transfer whose structures are known.[39] They are the essential components of our newly developed oxo transfer analogue reaction system.[17]

Mo(V) μ-Oxo Dimer Formation. Because of the lack of evidence for binuclear centers in oxotransferases, reactions mediated by them are unacceptable under the current oxo transfer hypothesis. Inasmuch as several Mo^{V}₂O₃ complexes have been reported to effect substrate reduction by oxo transfer,[40,41] it becomes obligatory to provide clear evidence that such a species is not involved in the analogue reaction systems described below. Shown in Figure 8 are the quantitative absorption spectra of MoO₂(tBuL-NS)₂ (yellow) and MoO(tBuL-NS)₂ (brown) and the spectrum of exactly equimolar mixtures of these two complexes, all in benzene solutions. The latter solution is intensely blue and possesses absorption bands at 560 and 635 nm, not found in the other complexes. We assign the blue chromophore as Mo₂O₃(tBuL-NS)₄, formed in the equilibrium reaction 3. μ-Oxo Mo(V) species of this sort invariably have absorption bands in the vicinity of 500 nm and, with sulfur ligands, are often purple

(35) Pickett, C.; Kumar, S.; Vella, P. A.; Zubieta, J. *Inorg. Chem.* **1982**, *21*, 908.

(36) (a) [MoO(Q₄)₂]²⁻, Q = S, Se: Draganjac, M.; Simhon, E. D.; Chan, L. T.; Kanatzidis, M.; Baenziger, N. C.; Coucouvanis, D. *Inorg. Chem.* **1982**, *21*, 3321. Wardle, R. W. M.; Mahler, C. H.; Chau, C.-N.; Ibers, J. A. *Inorg. Chem.* **1988**, *27*, 2790. (b) [MoO(S₂C₂O₂)₂]²⁻: Menneman, K.; Mattes, R. *J. Chem. Res. (M)* **1979**, 1372. (c) [MoO(S₂CₙH₄)₂]²⁻: Boyde, S.; Ellis, S. R.; Garner, C. D.; Clegg, W. *J. Chem. Soc., Chem. Commun.* **1986**, 1541. (d) [MoO(C₃S₅)₂]²⁻: Matsubayashi, G.-E.; Nojo, T.; Tanaka, T. *Inorg. Chim. Acta* **1988**, *154*, 133. (e) MoO(mnt)(dppe): Nicholas, K. M.; Khan, M. A. *Inorg. Chem.* **1987**, *26*, 1633. (f) MoO(S₂CNPr₂)₂: Ricard, L.; Estienne, J.; Karagiannidis, P.; Toledano, P.; Fisher, J.; Mitschler, A.; Weiss, R. *J. Coord. Chem.* **1974**, *3*, 277. (g) [MoO(Te₂C₂(COOMe)₂)₂]²⁻: Flomer, W. A.; Kolis, J. W. *Inorg. Chem.* **1989**, *28*, 2513. (h) MoO(S₂CPh)(S₃CPh): Tatsumisago, M.; Matsubayashi, G.; Tanaka, T.; Nishigaki, S.; Nakatsu, K. *J. Chem. Soc., Dalton Trans.* **1982**, 121. (i) MoO(S₂CSiPr)₂: Hyde, J.; Venkatasubramanian, K.; Zubieta, J. *Inorg. Chem.* **1978**, *17*, 414. (j) MoO(S₂COiPr)-(S₂C(PMe₃)OiPr): Carmona, E.; Galindo, A.; Gutierrez-Puebla, E.; Monge, A.; Puerta, C. *Inorg. Chem.* **1986**, *25*, 3804. The examples cited in (h–j) are bis(chelate) complexes, but they are not strictly five-coordinate owing to a weak Mo–C interaction involving the central carbon atom in one chelate ring.

(37) Chatt, J.; Dilworth, J. R.; Schmutz, J. A.; Zubieta, J. *J. Chem. Soc., Dalton Trans.* **1979**, 1595.

(38) (a) Berg, J. M.; Hodgson, K. O. *Inorg. Chem.* **1980**, *19*, 2180. (b) Roberts, S. A.; Young, C. G.; Cleland, W. E., Jr.; Ortega, R. B.; Enemark, J. H. *Inorg. Chem.* **1988**, *27*, 3044.

(39) The structures of a W^{VI}O₂/W^{IV}O pair related by oxo transfer have recently been reported: Ueyama, N.; Oku, H.; Nakamura, A. *J. Am. Chem. Soc.* **1992**, *114*, 7310.

(40) Craig, J. A.; Harlan, E. W.; Snyder, B. S.; Whitener, M. A.; Holm, R. H. *Inorg. Chem.* **1989**, *28*, 2082.

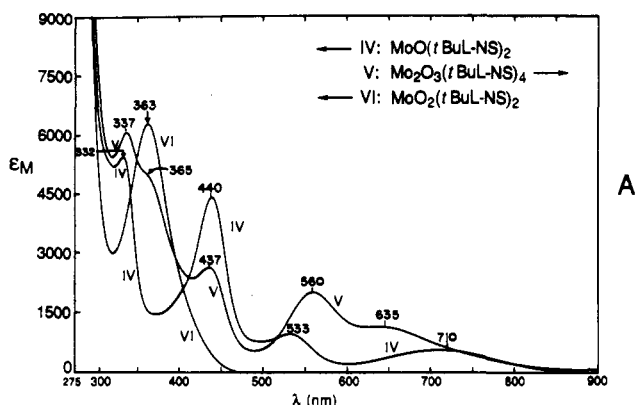(41) Baird, D. M.; Falzone, S.; Haky, J. E. *Inorg. Chem.* **1989**, *28*, 4562.

Figure 8. UV/visible absorption spectra of 2.21 mM solutions of MoO(tBuL-NS)$_2$ (IV) and MoO$_2$(tBuL-NS)$_2$ (VI) and the spectrum of Mo$_2$O$_3$(tBuL-NS)$_4$ (V) in equilibrium with IV and VI ([Mo]$_t$ = 5.53 mM). Spectra were recorded in benzene solutions at 25 °C. Absorption maxima are indicated; arrows refer to the extinction coefficient or absorbance axis.
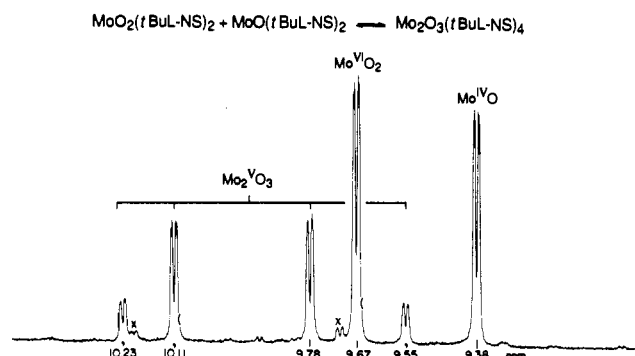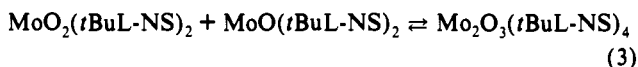
MoO$_2$(tBuL-NS)$_2$ + MoO(tBuL-NS)$_2$ ⟶ Mo$_2$O$_3$(tBuL-NS)$_4$

Figure 9. ^{1}H NMR spectrum (500 MHz) in the 6-H region of the indicated equilibrium mixture in which [MoO$_2$(tBuL-NS)$_2$]$_0$ = 20.1 mM and [MoO(tBuL-NS)$_2$]$_0$ = 17.8 mM. Signal assignments are indicated (x is an impurity); the ratio of the diastereomers of Mo$_2$O$_3$(tBuL-NS)$_4$ is 2.9:1.

or bluish in solution.[40]

$$\text{MoO}_2(t\text{BuL-NS})_2 + \text{MoO}(t\text{BuL-NS})_2 \rightleftharpoons \text{Mo}_2\text{O}_3(t\text{BuL-NS})_4$$
(3)

Further demonstration of the formation of the μ-oxo Mo(V) complex follows from the ^{1}H NMR spectrum in Figure 9. In this example, nearly equimolar amounts of MoO$_2$(tBuL-NS)$_2$ and MoO(tBuL-NS)$_2$ were equilibrated in benzene solution, and pyridyl 6-H resonances (Figure 1), which are the most sensitive to structure, were examined.[17] One 6-H signal each ($J_{HH} \approx 4$ Hz) is observed for the initial complexes owing to their C_2 symmetry. The remaining signals occur as two pairs whose components (at 9.55 and 10.23 ppm, and 9.78 and 10.11 ppm) possess exactly equal intensity and have a 2.9:1 intensity ratio. This pattern can only be explained by the formation of Mo$_2$O$_3$-(tBuL-NS)$_4$, which exists as two diastereomers (RS, RR + SS) because the half-molecules are chiral with inequivalent chelate rings. This is a particularly clear case of the detection of Mo$^V_2$O$_3$ diastereomers, and it is an example of one method for the detection of structures of this sort which we introduced earlier.[40] The structure of Mo$_2$O$_3$(tBuL-NS)$_4$ is expected to be analogous to other Mo$^V_2$O$_3$L$_4$ species[40] such as those with L = Et$_2$NCS$_2^-$ [36f] and N$_2$S$_2$ ligands.[42] From measurements of the concentration dependence of 6-H signal intensities, we find for reaction 3 in benzene that K_{eq} = 63(8) M^{-1} at 25 °C.

In donor solvents such as acetonitrile, THF, and DMF, blue colors have not been observed even in relatively concentrated solutions. We surmise that solvent association with Mo(IV)

(42) Dahlstrom, P. L.; Hyde, J. R.; Vella, P. A.; Zubieta, J. *Inorg. Chem.* **1982**, *21*, 927.
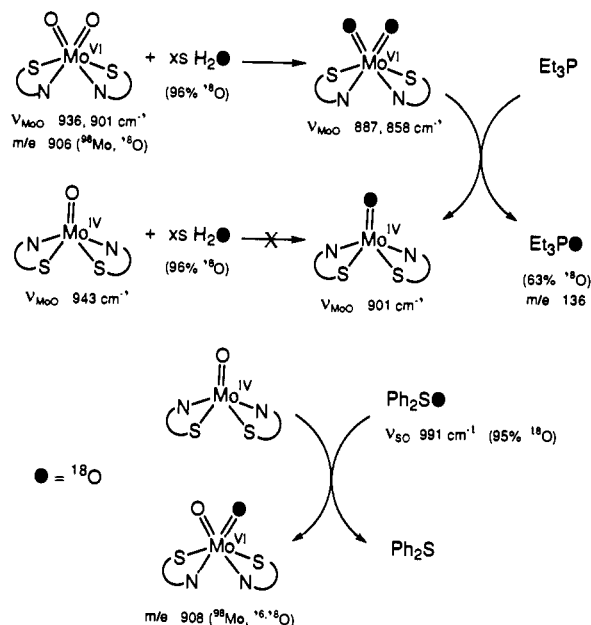

Figure 10. Scheme for the demonstration of oxygen atom transfer using ^{18}O labeling, including enrichment of MoO$_2$(tBuL-NS)$_2$ by reaction with trace [^{18}O]-H$_2$O, oxidation of Et$_3$P by enriched MoO$_2$(tBuL-NS)$_2$, and oxidation of MoO(tBuL-NS)$_2$ by 95% enriched Ph$_2$SO. All reactions were performed in THF solutions. Percent ^{18}O enrichments and Mo–O stretching frequencies are indicated.

together with steric effects suppresses μ-oxo bridge formation. When oxo transfer reactions of MoO$_2$(tBuL-NS)$_2$ and MoO-(tBuL-NS)$_2$ in DMF solutions are monitored spectrophotometrically or by ^{1}H NMR in the concentration regimes employed, no amount of Mo$_2$O$_3$(tBuL-NS)$_4$ could be detected. Hence, it is highly improbable that this species mediates oxo transfer in the reaction systems that follow.

Oxo Transfer with ^{18}O Labeling. In order to demonstrate that the oxygen atoms transferred to or from substrate in the forward and reverse reactions 4 *originate* in the Mo^{VI}O$_2$ group and the

$$\text{MoO}_2(t\text{BuL-NS})_2 + \text{X} \rightleftharpoons \text{MoO}(t\text{BuL-NS})_2 + \text{XO}$$
(4)

oxidized substrate, respectively, and not from contaminating water, trace dioxygen, or solvent, a series of ^{18}O-labeling experiments were performed. While other ^{18}O-labeled Mo^{VI}O$_2$, Mo^{IV}O, and Mo$^V_2$O$_{3,4}$ complexes have been prepared,[43] no oxo transfer reactions in which labels were monitored have been carried out previously. The reaction scheme is shown in Figure 10. All reactions were carried out in THF solutions; molybdenum complexes were identified by their ^{1}H NMR spectra (Figure 9). MoO$_2$(tBuL-NS)$_2$ was doubly labeled by reaction with trace H$_2^{18}$O and was isolated; the compound showed new ν_{MoO} stretches at 887 and 858 cm^{-1}. Its reaction with 1.0 equiv of Et$_3$P was carried to 93% completion; EI-MS analysis of the product showed it to be 63% Et$_3$P^{18}O.[44]

In a further experiment, MoO(tBuL-NS)$_2$ was treated with 1.1 equiv of Ph$_2$S^{18}O and the reaction was allowed to proceed to 95% completion. The residue from solvent removal was extracted with pentane and then ether, and the MoO$_2$(tBuL-NS)$_2$ product

(43) Newton, W. E.; McDonald, J. W. *J. Less-Common Met.* **1977**, *54*, 51.

(44) Less than complete enrichment of labeled substrate may arise from trace H$_2^{16}$O in media used to prepare labeled Mo^{18}O$_2$(tBuL-NS)$_2$ and for the reaction with Et$_3$P, and present in glassware and syringes. While the IR spectrum indicated substantial if not complete conversion to the doubly-labeled Mo^V^{18}O$_2$ complex, small quantities of mono-labeled or unlabeled complexes cannot be eliminated. We attempted to determine the enrichment of this complex by FAB-MS. We were able to detect but not to quantitate Mo^{18}O$_2$(tBuL-NS)$_2$ owing to extensive fragmentation under FAB conditions and the complicated isotope patterns (dominated by ^{16,18}O and seven Mo isotopes). (Subsequently, we were able to quantitate the mono-labeled complex by FD-MS, which gave only minimal fragmentation.)
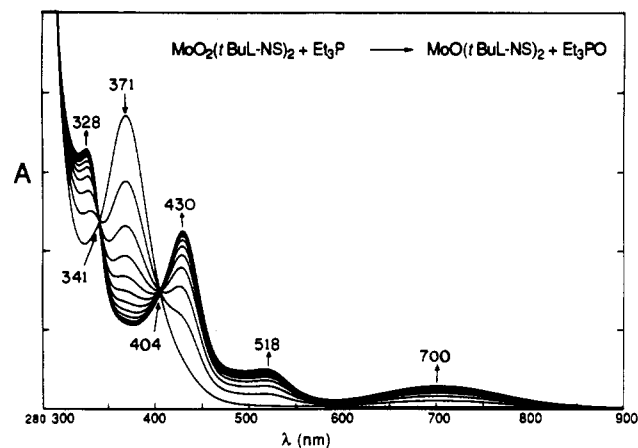
Figure 11. UV/visible spectral changes in the oxidation of Et$_3$P by MoO$_2$(tBuL-NS)$_2$ (λ_{max} 371 nm) in DMF solution at 22 °C. In this reaction, [MoO$_2$(tBuL-NS)$_2$]$_0$ = 1.07 mM and [Et$_3$P]$_0$ = 33.8 mM.

Figure 12. UV/visible spectral changes in the reduction of Ph$_3$AsO by MoO(tBuL-NS)$_2$ (λ_{max} 328, 430, 518, 700 nm) in DMF solution at 22 °C.

was examined by FD-MS. In the unlabeled compound, the peak with m/e 906 (^{98}Mo, 24.1% abundance) is the most intense; a weaker peak at m/e 908 is also observed. The spectrum of the reaction product contained a peak of enhanced intensity at m/e 908 and an overall intensity pattern across the isotope distribution which is consistent with the formation of 60% monolabeled product. In this case as well, back-exchange with trace H$_2^{16}$O has reduced the amount of labeled product. However, in both systems the point is proven: the isotope label has been transferred.

These experiments clearly demonstrate the origin of the oxygen atoms that are transferred to and from substrate. For reasons of comparison to our previous systems,[10-14,40] the substrate reactions described in the following section were carried out in DMF solutions. We have not performed ^{18}O-labeling experiments in DMF because of practical problems associated with the separation of small quantities of labeled substrates and complexes from this polar, high-boiling solvent. However, we have shown that the same reactions proceed in THF and DMF solutions. Thus, the reactions of MoO$_2$(tBuL-NS)$_2$ with excess Et$_3$P (23 equiv) and MoO(tBuL-NS)$_2$ with excess Ph$_2$SO (27 equiv) in THF solutions proceed to completion with respect to the molybdenum reactants. Absorption maxima and isosbestic points are essentially the same as in the DMF systems.

Substrate Reactions. The oxo transfer conversions of some 15 substrates, listed in Figure 3, have been examined in the forward and reverse reactions 4 carried out in DMF solutions. In the only example of oxo transfer to substrate, X = Et$_3$P was oxidized to Et$_3$PO in the reaction system monitored spectrophotometrically in Figure 11. The absorption band of the initial complex at 371 nm diminishes in intensity as the reaction proceeds, and features at 328, 430, 518, and 700 nm emerge. Tight isosbestic points are developed at 341 and 404 nm. The final spectrum is identical with that of MoO(tBuL-NS)$_2$ measured separately. In the reverse reaction, oxo transfer from substrate XO = Ph$_3$AsO, the reciprocal spectral changes in Figure 12 are observed. These examples are typical of reactions of the substrates in Figure 3 and demonstrate clean conversion to products. Yields are derived mainly from systems with mole ratios MoO(tBuL-NS)$_2$:XO of ca. 1:1 and were determined spectrophotometrically for most reactions, or otherwise by integration of 6-H resonances of initial and product complexes.[17]

We have previously introduced a thermodynamic scale of oxo transfer reactivity based on the generalized reaction in Table V.[8] In this scale, the oxidized member of the couple X/XO is thermodynamically competent to oxidize the reduced member of the couple Y/YO with a smaller ΔH. Elsewhere, we have recently provided a full account of this scale, which has been considerably expanded over the original.[45] That portion of the scale which
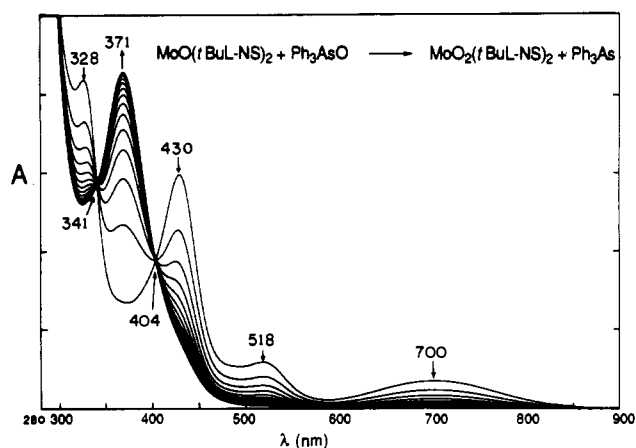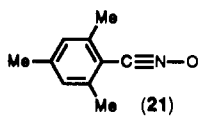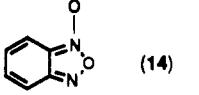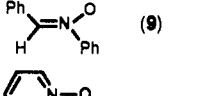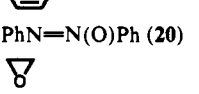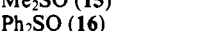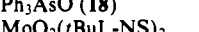
Table V. Thermodynamic Reactivity Scale and X–O Bond Energies for X(g) + $^1/_2$O$_2$(g) → XO(g)

XO	$\Delta H_{X/XO}{}^a$	$D_{X-O}{}^{a,b}$	ref
Me—⟨⟩—C≡N—O (21) (Me, Me, Me substituents)	+6.4	53	46
(14) (benzofurazan N-oxide)	−0.4	60	47
Ph—CH=N(O)—Ph (9)	−3.8	63	48
⟨⟩N—O (pyridine N-oxide)	−12.6	72	49
PhN=N(O)Ph (20)	−17.3	77	48
⟨⟩ (oxirane)	−25.1	81	50
Me$_2$SO (15)	−27.1	87	51
Ph$_2$SO (16)	−29.7	89	51
Ph$_3$AsO (18)	−43.1	103	52
MoO$_2$(tBuL-NS)$_2$	<−43		c
Me$_2$SO$_2$	−48.4	108	51
Me$_3$PO	−79.7	139	53

^{a} Units, kcal/mol. ^{b} $D_{X-O} = -\Delta H_{X/XO} + \Delta_f H°_m(O(g))$; the latter value is 59.55 kcal/mol. ^{c} This work.

contains the available data[46-53] for substrates examined in this work is contained in Table V. The observed reduction of Ph$_3$AsO immediately requires that ΔH for the MoO(tBuL-NS)$_2$/MoO$_2$(tBuL-NS)$_2$ couple be less than −43 kcal/mol but more than ca. −80 kcal/mol inasmuch as Et$_3$P reduces the Mo(VI) complex. This result further indicates that MoO(tBuL-NS)$_2$ should oxidize all substrates with ΔH > −43 kcal/mol, a prediction

(45) Holm, R. H.; Donahue, J. P. *Polyhedron* **1993**, in press. Because ΔG values parallel ΔH values for gas-phase reactions, the more extensive ΔH data base may be reliably used to order reactivities of the couples X/XO.

(46) Acree, W. E., Jr.; Tucker, S. A.; Zvaigzne, A. I.; Yang, M.-Y.; Pilcher, G.; Ribeiro da Silva, M. D. M. C. *J. Chem. Thermodyn.* **1992**, *24*, 213.

(47) Leitao, M. L. P.; Pilcher, G.; Acree, W. E., Jr.; Zvaigzne, A. I.; Tucker, S. A.; Ribeiro da Silva, M. D. M. C. *J. Chem. Thermodyn.* **1990**, *22*, 923.

(48) Kirchner, J. J.; Acree, W. E., Jr.; Pilcher, G.; Li, S. *J. Chem. Thermodyn.* **1986**, *18*, 793.

(49) Li, S.; Pilcher, G. *J. Chem. Thermodyn.* **1988**, *20*, 463.

(50) *The NBS Tables of Chemical Thermodynamic Properties*; Lide, D. R., Ed.; American Chemical Society and the American Institute of Physics: Washington, D.C.; *J. Phys. Chem. Ref. Data* **1982**, *11*, Supplement No. 2.

(51) Herron, J. T. In *The Chemistry of Sulfones and Sulfoxides*; Patai, S., Rappoport, Z.; Stirling, C. J. M., Eds.; Wiley: New York, 1988; Chapter 4.

(52) Barnes, D. S.; Burkinshaw, P. M.; Mortimer, C. T. *Thermochim. Acta* **1988**, *131*, 107.

(53) Cox, J. D.; Pilcher, G. *Thermochemistry of Organic and Organometallic Compounds*; Academic Press: New York, 1970; pp 478–482.

that is largely correct. Thus, this complex reduces a Se-oxide (**17**), two S-oxides (**15, 16**), benzofuroxan (**14**), adenine 1-oxide (**13**), pyridine N-oxides (**11, 12**), nitrones (**9, 10**), and tertiary amine N-oxides (**6–8**). This complex also reduces $NaIO_4$ in essentially quantitative yield.

Other systems containing $MoO(tBuL\text{-}NS)_2$ in DMF at room temperature were also examined similarly. Azoxybenzene (**20**) did not react over 2 days; $(MeO)_2SO_2$ caused some decomposition without giving an identifiable product. 2,4,6-Trimethylbenzonitrile N-oxide (**21**), m-chloroperoxybenzoic acid, styrene oxide, 1,2-epoxybutane, nitrate, and biotin S-oxide did react but the absorption spectrum of the product(s) did not correspond to clean formation of $MoO_2(tBuL\text{-}NS)_2$. In systems containing MoO_2-$(tBuL\text{-}NS)_2$, $(MeO)_2SO$ at 50 °C for 2 days caused only a slight diminution of the peak at 371 nm, and $Na_2SO_3/18$-crown-6 effected slow decomposition of the initial complex without any evident formation of $MoO(tBuL\text{-}NS)_2$. The reactivity scale in Table V indicates that the foregoing substrates, with the possible exception of $(MeO)_2SO_2$, are susceptible to oxo transfer. Evidently, other reactions wholly or in part intervene. Nitrate and sulfite are not included in the scale because reliable ΔH data are available only for aqueous solution. We have previously demonstrated reduction of nitrate by $Mo^{IV}O$ complexes in other systems.[14,40] Thus far, the oxidation of sulfite to sulfate mediated at a $Mo^{VI}O_2$ center has not been realized in any system.

Summary. The following are the principal findings and conclusions of this investigation.

1. A series of sterically hindered bidentate N–O and N–S ligands and their $Mo^{VI}O_2$ and $Mo^{IV}O$ complexes have been prepared. The ligand of choice in promoting oxo transfer reactivity, $(tBuL\text{-}NS)^-$, is readily prepared in high yield from commercial precursors.

2. A new oxo transfer reaction system based on the structurally defined complexes $MoO_2(tBuL\text{-}NS)_2$ (distorted octahedral) and $MoO(tBuL\text{-}NS)_2$ (distorted trigonal bipyramidal) has been developed. Ligand steric properties, which afford frontside hindrance of the $Mo^{VI}O_2$ group, eliminate the complicating feature of μ-oxo Mo(V) dimer formation in the concentration ranges and solvents utilized in oxo transfer.[54] However, $Mo^V_2O_3(tBuL\text{-}NS)_4$ in an equilibrium mixture with $MoO_2(tBuL\text{-}NS)_2$ and $MoO(tBuL\text{-}NS)_2$ can be generated in benzene solution.

3. With use of $Mo^{18}O_2(tBuL\text{-}NS)_2$ and $Ph_2S^{18}O$, a typical reducible substrate that has been labeled, it has been demonstrated that the oxygen atoms that are transferred to and from substrate originate in the $Mo^{VI}O_2$ group and the oxidized substrate, respectively.

4. The foregoing substrate limitations notwithstanding, in terms of substrate type this oxo transfer system is the most versatile yet demonstrated. It has been shown to transform cleanly a set of 15 substrates which include the following types: tertiary phosphine, As-oxide, Se-oxide, S-oxide, and a variety of N-oxides including pyridine and other heterocyclic N-oxides, nitrones, and tertiary amine oxides. These include five examples of enzyme substrates. $MoO(tBuL\text{-}NS)_2$ is thermodynamically competent to reduce all substrates with $\Delta H \geq -43$ kcal/mol on the reactivity scale, or with $D_{X-O} \leq 103$ kcal/mol.

5. Compared to the previous system based on MoO_2-$(L\text{-}NS_2)/MoO(L\text{-}NS_2)(DMF)$,[4,10–14] the current system offers

considerable advantages: (a) a structurally authenticated $Mo^{IV}O$ component; (b) good solubility properties in a range of coordinating and noncoordinating solvents, including DMF, Me_2SO, THF, CH_2Cl_2, toluene, and benzene; (c) stability to and reactivity with a much wider range of oxidized substrates,[55] including the strong oxo donors periodate and tertiary amine oxides; and (d) sensitivity of rates and activation parameters to differences in substrate. Certain examples of the latter point are noted elsewhere.[17]

In addition to present and past work in this laboratory,[4,10–15,17] a number of other molybdenum-mediated oxo transfer systems have been devised,[4,8,38b,55,56] although usually with limited substrates and uncharacterized $Mo^{IV}O$ species, and sometimes including oxo–Mo(V) intermediates. It is now clear that the enzyme substrates nitrate, S-oxides, aromatic N-oxides, and tertiary amine N-oxides can be reduced in clean reactions mediated at a $Mo^{IV}O$ center. These results provide strong support for the oxo transfer hypothesis as applied to enzymes whose active centers do not contain terminal sulfide or hydrosulfide ligands. Sulfite remains the one substrate of these that has not been transformed (to sulfate) by molybdenum-mediated oxo transfer.

In ongoing work, we are investigating the kinetics and mechanism of substrate oxidation and reduction using the oxo transfer system described here.[57] Beyond this work, it is clear that meaningful analogue reaction systems of the oxotransferases must involve mono-dithiolene molybdenum complexes, preferably close synthetic approaches to the molybdenum cofactor, or the cofactor itself. Lastly, it should be borne in mind that the steps of substrate transformation are only part of the enzymatic reaction cycle. The remaining part, whereby the oxidation states Mo(IV) ⟷ Mo(V) ⟷ Mo(VI) are traversed by correlated electron–proton transfer steps, has been incisively represented in a synthetic system by the seminal studies of Wedd and co-workers.[58] In related work, Xiao et al.[59] have reported a model system in which both atom and electron transfer steps are demonstrated.

Supplementary Material Available: Listings of crystal and intensity collection data, atom positional and thermal parameters, interatomic angles, and distances (28 pages); tables of calculated and observed structure factors (86 pages). Ordering information is given on any current masthead page.

(54) Sterically hindered oxomolybdenum complexes potentially useful in oxo transfer have been prepared in other laboratories, but detailed characterizations of structures and reactions have been confined to $Mo^{VI}O_2$ species: [14b] (a) Subramanian, P.; Spence, J. T.; Ortega, R. B.; Enemark, J. H. *Inorg. Chem.* **1984**, *23*, 2564. (b) Hinshaw, C. J.; Spence, J. T. *Inorg. Chim. Acta* **1986**, *125*, L17. (c) Sanz, V.; Picher, T.; Palanca, P.; Gómez-Romero, P.; Llopis, E.; Ramirez, J. A.; Beltrán, D.; Cervilla, A. *Inorg. Chem.* **1991**, *30*, 3113. (d) Llopis, E.; Doménech, A.; Ramirez, J. A.; Cervilla, A.; Palanca, P.; Picher, T.; Sanz, V. *Inorg. Chim. Acta* **1991**, *189*, 29.

(55) The $MoO_2(S_2CNEt_2)_2/MoO(S_2CNEt_2)_2$ system has considerable breadth of substrate reactivity: (a) Lu, X.; Sun, J.; Tao, X. *Synthesis* **1982**, 185. (b) Tanaka, K.; Honjo, M.; Tanaka, T. *Inorg. Chem.* **1985**, *24*, 2662. (c) Moloy, K. G. *Inorg. Chem.* **1988**, *27*, 677. However, the occurrence of the reaction $MoO_2(S_2CNEt_2)_2 + MoO(tBuL\text{-}NS)_2 \rightarrow MoO(S_2CNEt_2)_2 + MoO_2(tBuL\text{-}NS)_2$ in DMF and 1,2-dichloroethane, demonstrated by UV/ visible and ¹H NMR spectra, shows that of the two $Mo^{IV}O$ complexes, $MoO(tBuL\text{-}NS)_2$ is the stronger oxo acceptor. Because of the formation of $Mo_2O_3(S_2CNEt)_4$ in these systems, oxo transfer kinetics are complicated but have been analyzed:[15] (d) Unoura, K.; Kato, Y.; Abe, K.; Iwase, A.; Ogino, H. *Bull. Chem. Soc. Jpn.* **1991**, *64*, 3372.

(56) (a) Kaul, B. B.; Enemark, J. H.; Merbs, S. L.; Spence, J. T. *J. Am. Chem. Soc.* **1985**, *107*, 2885. (b) Nakamura, A.; Ueyama, N.; Okamura, T.; Zaima, H.; Yoshinaga, N. *J. Mol. Catal.* **1989**, *55*, 284. (c) Ueyama, N.; Yoshinaga, N.; Nakamura, A. *J. Chem. Soc., Dalton Trans.* **1990**, 387. (d) Roberts, S. A.; Young, C. G.; Kipke, C. A.; Yamanouchi, K.; Carducci, M.; Enemark, J. H. *Inorg. Chem.* **1990**, *29*, 3650. (e) Ueyama, N.; Yoshinaga, N.; Okamura, T.; Zaima, H.; Nakamura, A. *J. Mol. Catal.* **1991**, *64*, 247. (f) Bhattacharjee, S.; Bhattacharyya, R. *J. Chem. Soc., Dalton Trans.* **1992**, 1357.

(57) Schultz, B. E.; Holm, R. H., results to be published.

(58) Wilson, G. L.; Greenwood, R. J.; Pilbrow, J. R.; Spence, J. T.; Wedd, A. G. *J. Am. Chem. Soc.* **1991**, *113*, 6803.

(59) Xiao, Z.; Young, C. G.; Enemark, J. H.; Wedd, A. G. *J. Am. Chem. Soc.* **1992**, *114*, 9194.